A path integral Monte Carlo study of liquid neon and the quantum effective pair potential[a)]

D. Thirumalai, Randall W. Hall, and B. J. Berne

Department of Chemistry, Columbia University, New York, New York 10027

The path integral Monte Carlo (PIMC) method is used to simulate liquid neon at $T = 40$ K. It is shown that quantum effects are not negligible and that when the quantum effective pair potential is used in a classical molecular dynamics simulation the results obtained for the radial distribution function agrees with that predicted by a full path integral Monte Carlo simulation. The validity of this procedure is further shown by comparing the results obtained by this method to experimental measurements of liquid neon at $T = 35$ K.

INTRODUCTION

Argon, krypton, and xenon all obey the law of corresponding states, whereas helium and neon do not.[1,2] The reason is that helium and neon display quantum effects at liquid state temperatures, whereas the other inert gases are essentially classical at their liquid state temperatures. Indeed, the quantum properties of helium give rise to superfluidity, while neon does not display such dramatic effects, quantum effects cannot be ignored. In this paper we present a computer simulation of quantum neon using several different approaches.

The problem of simulating quantum systems is receiving increasing attention. Early work focused on determining the ground state properties of Fermi and Bose liquids. A variational Monte Carlo method using Jastrow trial functions was developed by Kalos *et al.*,[3,4] and applied with considerable success to the study of the ground state of helium. Kalos[5] developed a Green's function Monte Carlo technique that is easily applied to Bose liquids, but has not yet been as successfully applied to Fermi systems.[6] These methods are restricted to zero temperature problems. At finite temperatures other methods are required. One method that is worth exploring is path integral Monte Carlo (PIMC).[7] This method was introduced several years ago, and offers several immediate advantages over other methods. The discretized path integral formulation of quantum statistical mechanics allows a quantum particle to be replaced by a polymer chain of classical particles with harmonic forces between nearest neighbors.[8] If exchange is ignored, then the quantum liquid is represented by a classical liquid containing polymer chains where each particle on any chain interacts with one and only one particle on each of the other polymer chains. Since this is a classical liquid, it can be simulated by simple Monte Carlo techniques. The problem can also be cast in a form which allows classical molecular dynamics techniques to be used,[9] but as we show elsewhere,[10] when applied to the neon dimer, molecular dynamics can be nonergodic. There are several problems connected with the PIMC. First the simulation is slowly convergent,[11,12] second, the estimator

used to determine the average energy has very large fluctuations,[13] and, third it is very difficult to treat particle exchange. Another method that has been proposed recently is based on the propagation of Gaussian wave packets.[14,15] This method appears to be very promising; nevertheless, no trustworthy simulation of simple quantum fluids has yet been done using wave packet dynamics.

Recently, we have developed a very rapidly convergent method for evaluating path integrals in systems of a few quantum degrees of freedom. This method is based on direct numerical matrix multiplication (NMM),[16] and does not have any inherent numerical fluctuations. We have applied this method to tunneling problems[17] and to the determination of an effective potential between two interacting quantum particles. In a recent publication[16] we conjectured that a simulation of a classical liquid with pair potential given by the above quantum effective potential might provide a reasonable approximation to the full quantum liquid. In this paper we implement this suggestion and compare it to a full Monte Carlo evaluation of the path integral. In addition, these results are compared with various semiclassical approximations. It is found that the quantum effective potential (QEP) gives good agreement for neon. Given this, WCA theory[18] was applied to the quantum effective potential. Although the effective potential is much softer than the Lennard-Jones potential, it appears that the repulsive part of the WCA potential can be well represented by an effective hard sphere potential and it is not surprising then that the WCA theory is quite successful when applied to this problem.

METHODOLOGY

We consider a system of N particles interacting with pair potential $u(r)$. In addition, we ignore the statistics due to the indistinguishability of the particles. (An estimate of the importance of exchange is given in the Appendix.) The Hamiltonian of the system is

$$H = \sum_{i=1}^{N} \frac{P_i^2}{2m} + \sum_{i>j} u(|\mathbf{r}_i - \mathbf{r}_j|)$$
$$= T + V, \tag{1}$$

where $u(r)$ is the LJ (12-6) potential with $\sigma = 2.75 A$ and $\epsilon/k_B = 35.8$ K. The central quantity of interest in the calculation

of equilibrium properties is the partition function

$$Q = \mathrm{Tr}\, e^{-\beta H} = \mathrm{Tr}\, [e^{-(\beta/P)H}]^P, \qquad (2)$$

where $\beta = (k_B T)^{-1}$, and Tr stands for the trace, P is an integer, and the last equality follows because H commutes with itself. With the aid of the Trotter formula,[19] Eq. (2) can be written as

$$Q = \lim_{P \to \infty} Q_P, \qquad (3)$$

where

$$Q_P = \mathrm{Tr}\left\{\left[\exp\left(-\frac{\beta}{2P}V\right)\exp\left(-\frac{\beta}{P}T\right)\exp\left(-\frac{\beta}{2P}V\right)\right]^P\right\}. \quad (4)$$

If P is chosen so that β/P is small then it can be shown that (in the coordinate representation) Q_P becomes

$$Q_P = (mP/2\pi\hbar^2\beta)^{3NP/2}\int d\mathbf{r}^{(1)}\cdots d\mathbf{r}^{(P)}e^{-\beta\Phi(\mathbf{r}^{(1)},\dots,\mathbf{r}^{(P)})}, \qquad (5)$$

where $\mathbf{r}^{(t)}$ denotes the collection of the coordinates of the N particles at the "time" t, i.e., $\mathbf{r}^{(t)} = (\mathbf{r}_1^{(t)},\mathbf{r}_2^{(t)}\cdots,\mathbf{r}_N^{(t)})$, and

$$\Phi(\mathbf{r}^{(1)},\mathbf{r}^{(2)},\dots,\mathbf{r}^{(P)}) = (mP/2\beta^2\hbar^2)\sum_{t=1}^{P}\sum_{j=1}^{N}(\mathbf{r}_j^{(t)} - \mathbf{r}_j^{(t+1)})^2$$

$$+ (1/P)\sum_{t=1}^{P}\sum_{i>j}u(|\mathbf{r}_i^{(t)} - \mathbf{r}_j^{(t)}|), \qquad (6)$$

where $\mathbf{r}^{(1)} = \mathbf{r}^{(P+1)}$. Although Eq. (6) becomes "exact" in the limit as $P \to \infty$, in practice one is forced to deal with finite P. When P is finite, Q_P looks like the classical partition function for a system of $N \times P$ classical particles. In this approximation the N-particle quantum system resembles a classical system where each quantum particle is represented by a "flexible" ring polymer consisting of P "beads." Each bead in a ring polymer interacts with the neighboring bead through a harmonic potential with the force constant $(mP/\beta^2\hbar^2)$. It is also important to note that the t th bead in one ring polymer interacts with only the t th bead in any other ring polymer. Perhaps it is worth remarking that the above form of Eq. (6) which follows from Eqs. (4) and (5) is called the primitive algorithm. It has been recognized (through an assortment of examples) that for quantum mechanical systems at low temperatures the number of beads P required to account for the quantum dispersion can become extremely large.[11,12,16,17] Therefore there have been efforts to devise techniques to improve upon the primitive algorithm, including both the variational treatment[12] and a renormalization group approach.[20] In some circumstances, umbrella sampling techniques can be used to reduce P.[21] In addition, efforts have been made to include higher order terms in the Trotter formula to obtain a more accurate "short time" approximation.[22] It will perhaps be necessary to resort to some of these techniques to simulate quantum many body systems. However, in this paper we do not address these important questions further.

EFFECTIVE POTENTIAL APPROACH

In a previous paper,[16] we conjectured that the quantum effective potential $W(r;\beta)$ (QEP) (to be described below) used in a classical computer simulation might adequately de-

scribe the quantum effects in many-body quantum systems. Let us consider two identical (Ne) atoms enclosed in a large but finite box. Since the Ne atoms are assumed to interact via the Lennard-Jones potential, the Hamiltonian can be separated into a center of mass and relative coordinates. As shown in Ref. 16, the Bloch equation for the Hamiltonian describing the relative motion can be solved using the numerical matrix multiplication method (NMM), giving the exact path integral in the primitive algorithm. It is then a simple matter to obtain the effective potential $W(r;\beta)$ defined by

$$W(r;\beta) \equiv -(1/\beta)\ln g(r), \qquad (7)$$

where $g(r)$ is the pair correlation function. For details of this procedure the reader is referred to Ref. 16.

Before considering the liquid it is useful to access the accuracy of path integral Monte Carlo (PIMC) for the calculation of $g(r)$. In particular we consider two Ne atoms interacting via a Lennard-Jones potential enclosed in a box of side 4σ at the temperature of 40 K. The exact pair correlation function $g(r)$ was calculated by evaluating $\rho(r,r';\beta)$ (the density matrix corresponding to the relative motion) by NMM.[16] The PIMC was performed for the Hamiltonian of the relative motion and $g(r)$ was evaluated using the method described in the text. The number of beads, P, used in the PIMC was 40, whereas P was taken to be 64 in the NMM method. After the system had equilibriated to the desired temperature, $g(r)$ was computed using 500 000 additional passes. In Fig. 1 the effective potential determined from PIMC is compared with that from NMM. This figure shows that PIMC deviates from QEP at $r/\sigma < 0.95$ where the number of counts is small and the error is therefore large. In Fig. 2 it can be seen that PIMC gives a reliable estimate of $g(r)$.

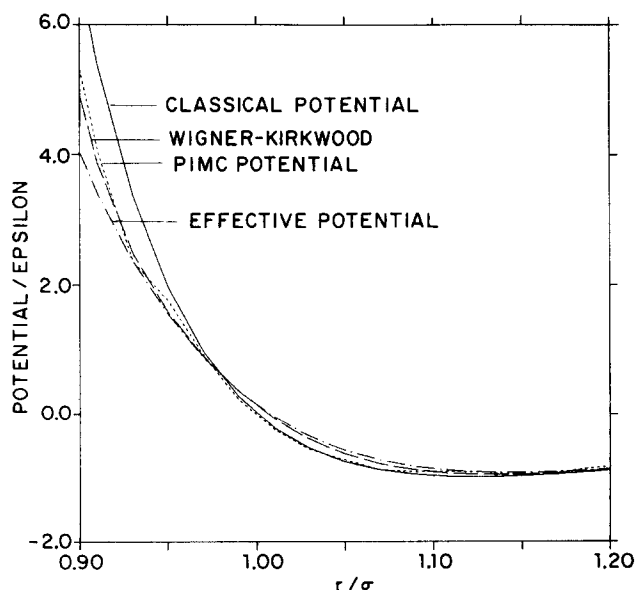For the sake of comparison we study two other pair

FIG. 1. Plot of the effective potential in units of ϵ as a function r/σ at $T = 40$ K. The solid line classical LJ potential; the dash line is the potential given by the Wigner–Kirkwood expansion [cf. Eq. (9)]; the dash–dot line represents the quantum effective potential given by Eq. (7); and the dotted line is the potential obtained by PIMC for two neon atoms enclosed in a box.
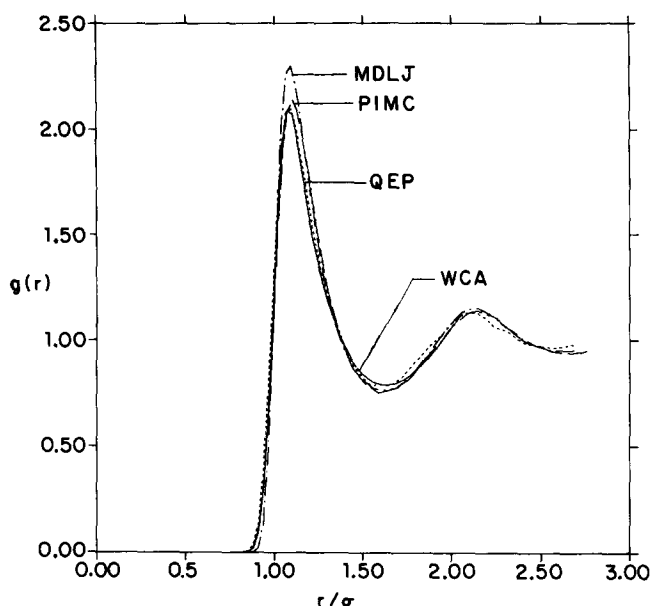
FIG. 2. The radial distribution function $g(r)$ as a function of r/σ for liquid neon at $T = 40$ K and $\rho\sigma^3 = 0.68$. The dashed line is the result of the PIMC simulation; the dotted line represents $g(r)$ obtained from a classical molecular dynamics simulation using the quantum effective potential; the dash-dot line is the result of the MDLJ simulation; the solid line is the prediction of the WCA theory using the QEP.

potentials which include quantum corrections to the classical LJ potential, namely,

$$W_{FH}(r;\beta) = V(r) + (\hbar^2\beta/24m)[V''(r) + (2/r)V'(r)] \quad (8)$$

and

$$W_{WK}(r;\beta) = V(r) - \beta^{-1}\ln\{1 - \{\hbar^2\beta^2/12m)$$
$$\times [V''(r)] + (2/r)V'(r) - (\beta/2)[V'(r)]^2\}. \quad (9)$$

The potential W_{FH} results from keeping only quadratic fluctuations around the classical path in the path integral and is called the Feynman–Hibbs potential.[23] The potential W_{WK} $(r;\beta)$ results from the leading terms in the Wigner–Kirkwood expansion of the partition function.[24,25]

In Fig. 1 we plot the classical (LJ) potential $V(r)$, the quantum effective potential $W(r;\beta)$ found using NMM and PIMC, and the Wigner–Kirkwood potential $W_{WK}(r;\beta)$ as a function of r/σ for $T = 40$ K. It can be seen that for such low temperatures $W(r;\beta)$ and $W_{WK}(r;\beta)$ are significantly softer than $V(r)$ [and $W_{FH}(r;\beta)$ although not shown in Fig. 1], indicating the importance of tunneling into the classically forbidden region. The minimum of $W(r;\beta)$ is at a higher value than the classical minimum. For $r/\sigma < 1$ $W_{FH}(r;\beta)$ is more repulsive than the classical potential. The potentials W_{WK} $(r;\beta)$ and $W(r;\beta)$ are remarkably similar for $r/\sigma > 0.93$. For $r/\sigma < 0.93$, $W_{WK}(r;\beta)$ is slightly more repulsive than $W(r;\beta)$ and for $r > 1.17\sigma$ both $W_{WK}(r;\beta)$ and $W(r;\beta)$ are virtually identical. This suggests that the leading $\hbar$ correction to the classical potential $V(r)$ as given by the Wigner–Kirkwood expansion of the partition function is adequate at this temperature. It will be necessary to calculate $W(r;\beta)$ using NMM [which includes corrections to $V(r)$ to essentially all orders of $\hbar$], only when the Wigner–Kirkwood approximation indicates strong quantum corrections. However, the Wigner–Kirkwood potential [Eq. (9)] is an asymptotic ex-

pansion in powers of $\hbar$ and, thus, care should be exercised in inverting the partition function to obtain the effective potential. In particular one might think that the partition function can be expressed as

$$Q \sim \int dr \exp - \beta \left\{ V(r) + \frac{\hbar^2\beta}{12m}\left[V''(r) \right. \right.$$
$$\left. \left. + \frac{2}{r}V'(r) - \frac{\beta}{2}[V'(r)]^2 \right] \right\}. \quad (10)$$

Unfortunately, one cannot be so cavalier with asymptotic expansions. In fact this gives very poor agreement with the effective potential. Instead one should use the Wigner–Kirkwood potential given by Eq. (9).

WCA ANALYSIS USING THE QUANTUM EFFECTIVE POTENTIAL

In this section we examine the efficacy of the modern van der Waals theory of liquids (WCA theory)[18] to calculate the radial distribution of Ne using the quantum effective pair potential $W(r;\beta)$ defined in Eq. (7) and displayed in Fig. 1. For completeness a brief sketch of WCA theory is given. According to WCA theory,[18] the interparticle potential is written as the sum of a purely repulsive part $W^{(0)}(r;\beta)$ and a purely attractive part $W^{(1)}(r;\beta)$, i.e.,

$$W(r;\beta) = W^{(0)}(r;\beta) + W^{(1)}(r;\beta), \quad (11)$$

where

$$W^{(0)}(r;\beta) = \begin{cases} W(r;\beta) + \Delta & r < r_m, \\ 0 & r > r_m, \end{cases}$$

and

$$W^{(1)}(r;\beta) = \begin{cases} -\Delta & r < r_m, \\ W(r;\beta) & r > r_m. \end{cases}$$

In Eq. (11), r_m is the distance at which the repulsive force becomes zero and $\Delta = W(r_m;\beta)$.

In the WCA approximation $g(r)$ is approximated by

$$g(r) \simeq g^{(0)}(r), \quad (12)$$

where $g^{(0)}(r)$ is the radial distribution function for a fluid with the repulsive pair potential $W^{(0)}(r;\beta)$. $g^{(0)}(r)$ is then approximated by

$$g^{(0)}(r) \cong y_{HS}(r;d)e^{-\beta W^{(0)}(r;\beta)}, \quad (13)$$

where $y_{HS}(r,d)$ is the cavity distribution function of an "equivalent hard sphere fluid" with diameter d; where d is determined from

$$\int_0^d dr \, r^2 y_{HS}(r;d) = \int_0^\infty dr \, r^2 y_{HS}(r;d)[1 - e^{-\beta W^{(0)}(r;\beta)}], \quad (14)$$

the requirement that the compressibility of the equivalent hard sphere fluid is the same as that of the repulsive system $\{W^{(0)}(r;\beta)\}$.

COMPUTATIONAL DETAILS

Corbin and Singer[15] used an extension of the semiclassical wave packet method to simulate the properties of quantum neon at 40 K and a density $\rho\sigma^3 = 0.68$. They neglected exchange effects. We performed four calculations for this same system: (1) A classical molecular dynamics using the

Lennard-Jones potential $V(r)$ (MDLJ); (2) classical MD simulation using the Feynman–Hibbs potential, $W_{FH}(r;\beta)$ (MDFH) [cf. Eq. (8)]; (3) a classical MD simulation using the effective quantum potential $W(r;\beta)$ (QEP) [cf. Eq. (7)]; and, finally, (4) a full path integral Monte Carlo simulation (PIMC). In all these calculations we used 108 particles, with Lennard-Jones parameters $\sigma = 2.75$ Å and $\epsilon = 35.8$ K. In the path integral Monte Carlo (PIMC) simulation, 40 particle chains $(P = 40)$ were found to be adequate at this temperature. In terms of the usual reduced units,[26] the time increment was taken to be 0.016 in the classical MD simulations. The potential was spherically truncated and shifted at half the box length. In the case of the MD simulation using the LJ potential the equations of motion were integrated up to 2000 time steps with averages being performed over the last 1800 time steps. For the other two MD simulations, i.e., using $W_{FH}(r;\beta)$ and the $W(r;\beta)$ the trajectories were followed for 15 000 and 19 000 steps, respectively, and averages were performed after discarding the first 1000 steps. We note that for these long runs the computed $g(r)$'s are quite accurate. In the PIMC two parameters were used: the step size of the center-of-mass of each polymer chain (composed of $P = 40$ particles) was taken to be 0.18σ and the step size for the moves of the particles of each chain was taken to be 0.0186σ. Averages were performed over 5000 passes after the potential energy had equilibriated. The radial distribution function $g(r)$,

$$g(r) = \langle (1/P) \sum_{t=1}^{P} \delta(r_{ij}^{(t)} - r) \rangle,$$ (15)

was calculated using MDLJ, QEP, and PIMC and by applying WCA to $W(r;\beta)$. The results are shown in Fig. 1. The PIMC calculation is regarded as the exact result. The figure shows that at this temperature (40 K) quantum effects seem to be significant. The notable feature is the appearance of tunneling into the classically forbidden region. In addition, the height of the first peak of the PIMC result is a few percent lower than the corresponding (MDLJ) classical RDF. It should also be noted that for $r > 1.5\sigma$ the PIMC result and the (MDLJ) RDF are in very good agreement. The observation that the quantum effects for $g(r)$ become insignificant at large r has also been made recently by Powles and Abascal.[27] Within the numerical uncertainties of the simulations the RDF obtained by using QEP seems to be in quantitative agreement with the PIMC simulation. In particular, it correctly predicts the tunneling effects and the mild suppression of the height of the first peak. We also found that the RDF predicted from MDFH is more in agreement with the classical result MDLJ than with the PIMC calculations. This is not surprising since, from Eq. (8), the potential $W_{FH}(r;\beta)$ is more repulsive than the Lennard-Jones potential and the correction due to the zero point quantum motion is not of the same magnitude as the effective potential.

In Fig. 2 we also compare $g(r)$ as a function of r by applying the WCA theory to the quantum effective potential and the RDF calculated from the PIMC simulation. Although not shown in Fig. 2, when WCA theory is applied to $W_{FH}(r;\beta)$ it yields $g(r)$ which is in very good agreement with MDFH. The equivalent hard sphere diameter was calculated in all cases using the simple algorithm given by Verlet and
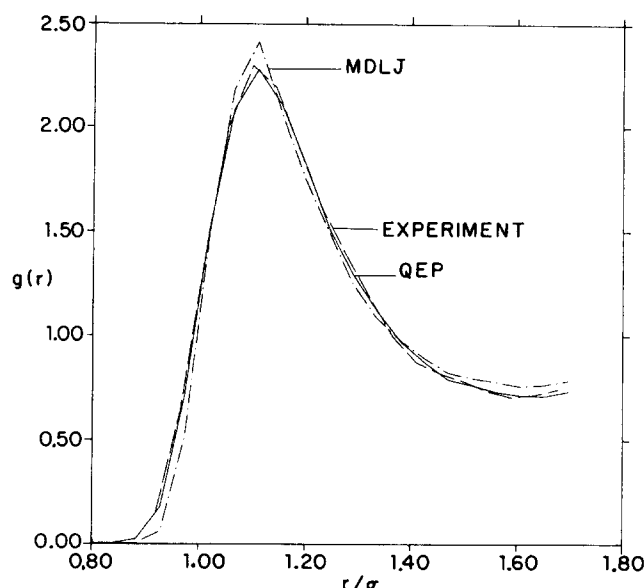

FIG. 3. The radial distribution function $g(r)$ as a function of r/σ for liquid neon at $T = 35.05$ K and $\rho\sigma^3 = 0.66$ where $r = 2.75$ Å. The solid line is the MD result using pure classical QEP; the dash–dot curve is obtained using MDLJ; the dash curve represents the experimental results of deGraaf and Moser as analyzed by Raveche and Mountain.

Weis.[28] All the required integrals were evaluated numerically. The parameters r_m and Δ for the effective potentials are 1.14σ and 0.93ϵ, respectively, whereas for the FH potential r_m is 1.13σ and Δ is 0.90ϵ. The hard sphere diameter calculated using the Verlet–Weis algorithm for the effective potential is 1.0084σ and for the FH potential the calculated value of d is 1.012σ. The application of WCA to QEP does compare well with the results of the PIMC simulation.

It has been shown that a classical system of neon atoms interacting through the effective pair potential $W(r;\beta)$ gives good agreement with the full path integral Monte Carlo simulation of neon atoms at $T = 40$ K and $\rho\sigma^3 = 0.68$. To further test the accuracy of classical simulations with the effective pair potential (QEP), we compare such simulations to the experimental $g(r)^{29,30}$ of liquid neon at $T = 35.05$ K and $\rho\sigma^3 = 0.66$. The parameters used to determine $W(r;\beta)$ from NMM were the same as before except for temperature, $T = 35.05$ K. Figure 3 shows a comparison between simulation and experiment for $g(r)$. The agreement is very good. Also included is the $g(r)$ from a simulation of neon interacting with a LJ (12-6) potential, under the same conditions. The purely classical (MDLJ) simulation does not account for tunneling and predicts a larger first peak. For $r > 1.6\sigma$ quantum effects cease to be important.

CONCLUSION

In this paper we report results of a simulation of liquid neon using the path integral Monte Carlo (PIMC) technique. Neon is assumed to interact with an LJ(12-6) potential. Our motivation for making this study was to test a previously made conjecture that the quantum effective pair potential could be used in a classical simulation. In this paper we have shown that this conjecture agrees with the full PIMC result.

It is also shown that the Wigner–Kirkwood asymptotic expansion also provides good agreement with $W(r;\beta)$, so that it can be used with some success in classical simulations. It is tempting to speculate that the quantum effective pair potential can be used to calculate dynamic correlation functions in quantum many body systems.

In the course of this study we found that PIMC for two interacting neon atoms agrees reasonably well with the results obtained with NMM, leading us to believe that PIMC gives accurate results for quantum liquids.

ACKNOWLEDGMENTS

APPENDIX

In this appendix we assess the importance of the exchange contribution due to the interchange of two particles. Consider two indistinguishable free particles of mass m enclosed in a box of volume V. The density matrix for the relative coordinate is

$$\rho(\mathbf{r}\,\mathbf{r}';\beta) = \left(\frac{\mu}{2\pi\hbar^2\beta}\right)^{\frac{3}{2}}\left[\exp\ -\frac{\mu}{2\hbar^2\beta}\,(\mathbf{r}-\mathbf{r}')^2\right.$$
$$\left.+\exp\ -\frac{\mu}{2\hbar^2\beta}\,(\mathbf{r}+\mathbf{r}')^2\right], \tag{A1}$$

where $\mathbf{r}$ denotes the relative coordinates of the two particles and μ is the reduced mass. The first term in Eq. (A1) is the direct contribution to $\rho(r,r';\beta)$ and the second term is due to exchange. When the particles are free, the exchange contribution to $\rho(r,r';\beta)$ becomes important only at low temperatures (large β) and small values of r. For two free neon atoms at $T=40$ K the exchange term decreases as $e^{-\alpha r^2}$ where $\alpha = 4.21\times10^{15}$. In particular, for r equal to the mean separation of atoms at $\rho\sigma^3 = 0.68$ the exchange contribution to $\rho(r,r;\beta)$ is 1.6% that of the direct contribution. When the particles interact via the Lennard-Jones potential the harsh repulsion at small distance will prevent any two particles from being close enough to each other for exchange to be important. Thus the presence of the potential would tend to decrease the exchange contribution relative to that of free particles, unless the temperature is much lower. This has

been numerically verified for two neon atoms in a box.[31] However, at higher densities the exchange contribution to $g(r)$ may become dominant. We believe that the exchange contribution to the interchange of three or more particles is less important than the two particle exchange.

[1]E. A. Guggenheim, J. Chem. Phys. 13, 253 (1945).

[2]J. P. Hansen and I. R. McDonald, *Theory of Simple Liquids* (Academic, London, 1976).

[3]M. H. Kalos, D. Levesque, and L. Verlet, Phys. Rev. A 9, 2178 (1974).

[4]For a review see C. E. Campbell, in *Progress in Liquid Physics*, edited by C. A. Croxton (Wiley, New York, 1978).

[5]For a review see D. M. Ceperley and M. H. Kalos, in *Monte Carlo Methods in Statistical Physics*, edited by K. Binder (Springer, Berlin, 1979).

[6]J. W. Moscowitz, K. E. Schmidt, M. A. Lee, and M. H. Kalos, J. Chem. Phys. 77, 349 (1982); K. E. Schmidt and M. H. Kalos (preprint).

[7](a) H. F. Jordon and L. D. Fosdick, Phys. Rev. 171, 128 (1968); (b) J. A. Barker, J. Chem. Phys. 70, 2914 (1979).

[8]R. P. Feynman, Rev. Mod. Phys. 20, 367 (1948).

[9]M. Parinello and A. Rahman, J. Chem. Phys. 80, 860 (1984).

[10]R. W. Hall and B. J. Berne, J. Chem. Phys. (in press).

[11]D. Chandler and P. G. Wolynes, J. Chem. Phys. 74, 4078 (1981).

[12]K. S. Schweizer, R. M. Stratt, D. Chandler, and P. G. Wolynes, J. Chem. Phys. 75, 1347 (1981).

[13]M. F. Herman, E. J. Bruskin, and B. J. Berne, J. Chem. Phys. 76, 5150 (1982).

[14]E. J. Heller, J. Chem. Phys. 62, 1544 (1975); 64, 63 (1976).

[15]N. Corbin and K. Singer, J. Phys. 46, 671 (1982).

[16]D. Thirumalai, E. J. Bruskin, and B. J. Berne, J. Chem. Phys. 79, 5063 (1983)

[17]D. Thirumalai and B. J. Berne (in preparation).

[18]J. D. Weeks, D. Chandler, and H. C. Andersen, J. Chem. Phys. 54, 5237 (1971).

[19]M. F. Trotter, Proc. Am. Math. Soc. 10, 545 (1959).

[20]G. Jongeward and P. G. Wolynes, J. Chem. Phys. 79, 3517 (1983).

[21]R. A. Friesner and R. H. Levy, J. Chem Phys. 80, 4488 (1984).

[22]H. DeRaedt and B. DeRaedt, Phys. Rev. A 28, 3575 (1983).

[23]R. P. Feynman and A. R. Hibbs, *Path Integrals and Quantum Mechanics* (McGraw–Hill, New York, 1965).

[24]E. Wigner, Phys. Rev. 40, 749 (1932).

[25]J. G. Kirkwood, Phys. Rev. 44, 31 (1933); see also R. M. Stratt, J. Chem. Phys. 72, 1685 (1980).

[26]L. Verlet, Phys. Rev. 139, 98 (1964).

[27]J. G. Powles and J. L. F. Abascal, J. Phys. C 16, L441 (1983).

[28]L. Verlet and J. Weis, Phys. Rev. A 5, 939 (1972).

[29]L. A. deGraaf and B. Mozer, J. Chem. Phys. 55, 4967 (1971).

[30]For a tabulation of $g(r)$ see H. J. Raveche and R. D. Mountain, J. Chem. Phys. 57, 3987 (1972).

[31]D. Thirumalai and B. J. Berne (unpublished results).